*This article is a non-peer reviewed preprint published at EarthArXiv*

# A New Mechanism for Terrace Formation in Submarine Canyons

Anjali M. Fernandes[1], David Mohrig[1], James Buttles[1],

[1] The Center for Integrative Geoscience, University of Connecticut, Storrs, Connecticut, USA.

[2] The Jackson School of Geosciences, The University of Texas at Austin, Texas, USA.

Email: anjali.fernandes@uconn.edu

**Deep canyons on Earth occur in both terrestrial and submarine environments, where they are carved by incising channels. Flights of apparently similar unpaired terraces, seen at the inside of bends in incised sinuous channels, are common in both environments. Here we demonstrate a new mechanism for terrace formation that we believe is unique to settings where sediment transporting flows are only slightly denser than the ambient fluid, such as those encountered in submarine environments or on other planets and moons. Whereas it is well known that variable rates of river incision and lateral migration create bedrock terraces in river canyons, the processes responsible for their submarine counterparts are largely unexplored (Fig.1), limiting our ability to reconstruct canyon evolution and therefore landscape history in these environments. Tangential momentum in turbidity currents traversing canyon bends can cause currents to run far up the outer banks of bends, such that flow separates from inner banks. The result is very little current and very low velocities along the channel bottom near the inside of the bends. We present experimental results that capture terrace formation at the inner banks of bends, through sustained erosion by energetic currents outside low-velocity, flow-separation zones coupled with no erosion or weak deposition within separation zones.**

On the Earth's surface, deep canyons (e.g. the Grand Canyon, ~1.83 km deep) present significant erosional relief, and are usually created as a result of river incision into an uplifting and eroding landscape in terrestrial environments; deep submarine canyons (e.g. Zhemchung Canyon, ~2.5 km deep) that dissect Earth's continental margins are also erosional, but incise into a depositional landscape. Although submarine canyons have been the primary conduits for sediment delivery from continental shelves to the deep oceans[1], the erosional mechanics associated with their formation are incompletely understood. Modern and ancient shelf margins contain the record of numerous erosional canyons, carved by turbidity currents and filled in by the deposits of oceanic sediment-transporting flows[2]. Whereas a significant fraction of the morphodynamic history of canyon filling can be assembled by querying the sedimentary record that results[3], elucidating the morphodynamics of canyon erosion is significantly more challenging, as the shape of a canyon represents the composite erosional imprint of numerous geomorphic states. On the modern seafloor, canyons are largely inactive today or challenging to access and instrument[4–7], and so capturing the temporal evolution of these landforms can be a formidable task.

A significant difference between terrestrial and submarine environments is the density of the transporting fluid relative to the density of the ambient fluid. In nature and the laboratory, turbidity currents have been observed to run up the outer walls of channel bends[8,9]. This occurs because the they have densities that are only slightly greater than the ambient water. This phenomenon has been shown to influence depositional patterns in submarine channels, specifically the development of bars at the outer banks of bends [9,10]. For decades, researchers have used physical experiments to study the dynamic interactions between turbidity currents and channels, at reduced spatio-temporal scales[9,11–15]. However, these experiments have focused on either purely depositional turbidity currents or erosional currents that mobilized in-channel sediment as bedload. The non-cohesive sediments used in these experiments possess properties that differ from sediment encountered by canyons incising into shelf margins. The cohesive, compacted or indurated, and generally fine-grained strata on shelf margins can only be entrained when a threshold for particle detachment is exceeded[16]. This “detachment-limited” erosion occurs when the shear stress exerted by the flow overcomes the cohesive strength of the sediment[17], at which point the fine particles are advected down-system into deeper water.

In our experiment we used a channel built of a cohesive mix of fine-grained acrylic sediment (specific gravity = 1.15) and kaolinite clay particles that were easy for laboratory-scale flows to suspend once detached, thereby replicating similar conditions to those encountered in actively eroding, detachment-limited submarine canyons. Specifically, we documented flow and sediment transport patterns associated with terrace formation at the inner banks of bends. Each density current produced net erosion, with detached material almost entirely advected out of the system in suspension (Fig. 2A). In our experiment, the run-up of low excess density currents against the outer walls of channel bends caused the flow to separate from the inner bank of the bend (Fig. 2.B, Fig. 3). Terraces formed within low-velocity flow-separation zones at channel bends. Terrace relief, relative to the lowest point of the channel, grew through accumulation of suspension deposits within the flow separation zone, and sustained erosion outside it along the pathway of the high-velocity core of the current. Flow through the separation zone displayed low sediment concentrations and velocities (~2 cm/s) low enough to permit sedimentation and preclude remobilization of deposited sediment; the highest velocities (>10 cm/s) and sediment concentrations were associated with the main current running up the outside of the bend (Fig. 2; Fig. 3).

Erosion in the channel occurred through wear by abrasion and plucking, evolving the channel bed and outer walls into ornate erosional bedforms in a manner similar that observed in detachment-limited bedrock rivers[17](Fig. 4). Erosional scour pits that initiated at the outer banks of bends grew and propagated downstream, eventually coalescing to form a deeply entrenched inner channel (Fig.1). The leading edges of these pits were sites of high turbulence and focused erosion. They intermittently released clouds of sediment particles that were transported downstream in suspension or aggregates of cohesive sediment that, dragged along by the flow, bounced and scraped along the channel before disintegrating into clouds of suspended sediment. Linear grooves that patterned the channel bed and outer walls of bends, oriented parallel to the direction of flow, were likely formed by the scraping of these aggregates against the bed (Fig. 3), although near-bed turbulence may also have contributed to their formation. Erosion of the channel bed was spatially discontinuous and followed the pathway of the high-velocity core of the current (Fig 1). Enhanced erosion occurred at sites where the channel bed was roughened through plucking or the intersection of linear grooves (Fig. 3).

Strath terraces, etched into bedrock by river incision, have long been recognized as recorders of former river bed elevations. Flights of unpaired terraces along the inner walls of bedrock river meanders, are commonly interpreted to be the result of non-steady lateral erosion or vertical incision rates. Intervals of predominant lateral erosion plane off bedrock terraces which slope gently towards the river channel; intervals of predominant vertical incision form the steep slopes that separate terraces. They sometimes display a thin layer of gravel or coarse bedload, augmented by floodplain deposition. Strath terraces are thought to form through varying rates of river incision or lateral erosion in response to one or more factors such as tectonic uplift, sea-level change, variability in climatically-modulated sediment supply, bedrock strength variability and local channel bed steepening following bend cut-off [18–23].

Terraces near the inner banks of incising submarine channels, similarly thought to record progressive incision and lateral migration, have been documented in a number of submarine channels and canyons[24–27]. We compared the cross-sectional shapes of incisional terrestrial and submarine channels/canyons, at or near their bend apices, to those that were dynamically evolved in our experiment (Fig. 5). To account for their very different scales, we divided local channel depth by the vertical distance between the top of the outer channel wall and the channel thalweg; cross-channel distance was divided by the length equal to the distance between the channel walls at the height of the outerwall. Intriguingly, in all submarine cases a similar percentage of the channel width is occupied by terraces at the insides of bends (50-60%), whereas the terrestrial cases show more variability (30%-70%). Whereas the variability in dimensionless width of inner channels at bend apices in the submarine channels is relatively small (40-50%), the local depth of inner channels compared to total channel relief is quite variable (30-60%). The striking similarities in cross-sectional shapes of natural and experimental incisional submarine channels suggests a degree of self-similarity in the processes that form these features, though the variability in the relative depth of the inner channels is likely due to differences in the incision rate or formation time.

Based on our experimental observations and the dimensionless comparisons, we propose that terraces can form at the insides of bends in submarine canyons when (a) turbidity currents do not fill the cross-sectional area of the canyon and the canyon is wide enough to permit the free meandering of the high velocity core of the current and (b) the outer wall slope is shallow enough to allow run-up of flow at the outside of bends and separation of flow from the inside. The erosional boundary of our experimental terraces coincided with the boundary of the flow separation zones; steep edges separating flights of terraces in natural submarine bends may mark the location of the shifting boundary of the flow separation zone as its shape changed in tandem with the outward erosion of the channel bend through time. Although variable relative rates of incision and lateral migration may, as in bedrock rivers, contribute to the formation of unpaired inner-bank terraces in submarine canyons, terraces may also form through the relatively simple and hitherto under-recognized process of flow separation from the inner bank. In contrast to strath terraces in river canyons, submarine separation-zone terraces will not be capped by bedload deposits, but by suspended load, as bedload transport will track the highest flow velocities and lowest topography towards the outside of the bend.

Furthermore, there can be important differences in the processes that act along the outer walls of canyons: although likely to be subject to hillslope processes in both environments, the outer walls of canyon bends may be significantly modified by turbidity currents at elevations accessible to through-going flows. Canyon walls may even display linear grooves, similar to those seen in our experiment, made by currents running up the outer walls of bends with low slopes. In remotely sensed environments (e.g. the deep ocean, the surfaces of other planets and moons, etc.), the presence of flow-parallel grooves high up on outer canyon walls will likely be diagnostic of extreme flow run-up at the outer walls. Therefore, in order to fully understand the process of canyon evolution, and the landscape history ciphered into canyon morphology, it is important to understand how the eroding flow is partitioned across the channel cross section.

In summary, our results demonstrate that unpaired submarine canyon terraces, though apparently similar in form to those encountered in terrestrial canyons, can be generated by significantly different processes. The formation mechanism of separation-zone terraces require extreme flow run-up at the outer bank and is thus unique to environments in which the eroding currents are only slightly denser than the ambient fluid. We therefore emphasize that the relative density of transporting flows must be taken into account when using canyon morphology to infer formative processes and landscape history in environments on Earth as well as other planets and moons.

## Figures & Captions

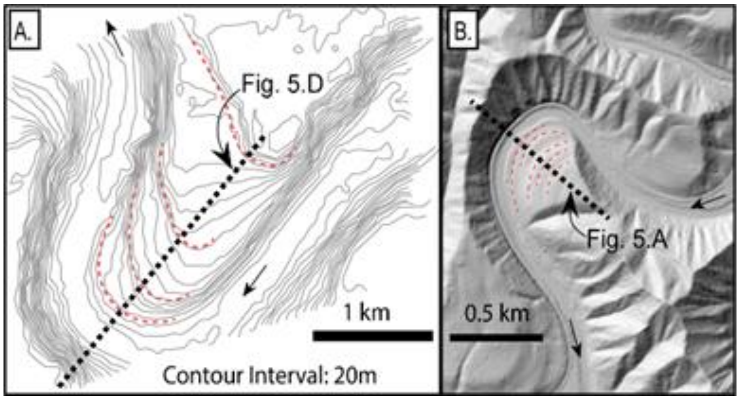


**Figure 1: A. Bathymetry map showing unpaired terraces at the inside of a bend in the Congo channel (modified from Babonneau et al., 2010). B. Hillshaded bare earth LiDAR map of a bend in the Smith River, showing flights of unpaired terraces at the inside of the bend.**

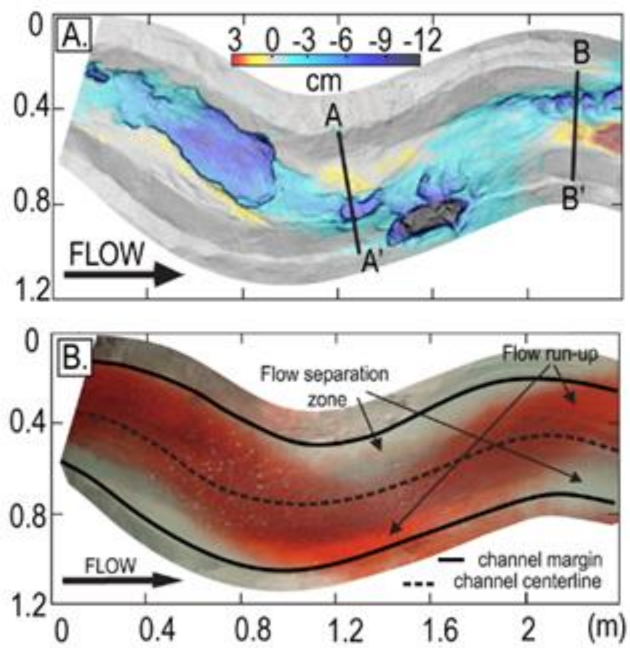


**Figure 2: A) A Map of elevation change from the passage of 5 density currents, draped over a slope map of the final channel. B) An overhead photograph showing the passage of a density current (dyed red) through the channel. The high-intensity red dye tracks the path of high velocities, while very little dyed current is apparent within low- velocity flow-separation zones at the inner banks of bends. Terraces in flow-separation zones grew in relief relative to the channel talweg through sustained erosion (cold hues) outside the separation zone and thin suspension deposition (warm hues) within it.**

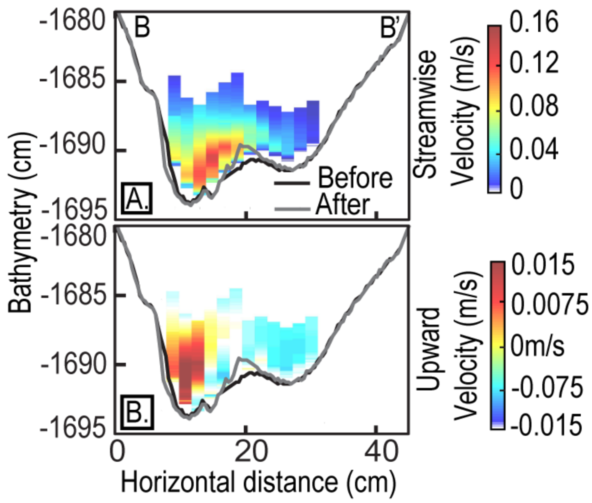


**Figure 3: Magnitudes of near-bed velocities, separated into (A) the bed-parallel, downstream component of velocity, and (B) upward directed velocity at cross section B-B' in Fig. 1, collected during the passage of a density current. The surface elevation at B-B' before and after the passage of the density current is shown here. Note the extremely low flow velocities over the terrace, tied to deposition. Upward directed velocities at the outside of the bend in (B) are related to flow run-up and increased turbulence from the rough, eroding bed.**

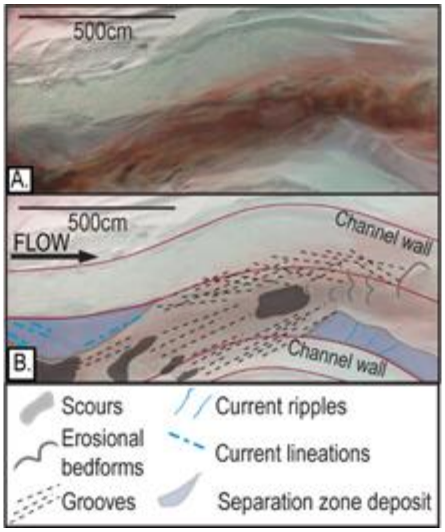


**Figure 4: A. Perspective view of the channel bed (through the water column) at the end of the experiment. B. Interpretive overlay indicating surface morphology associated with erosion in the inner channel and deposition on the terraces.**

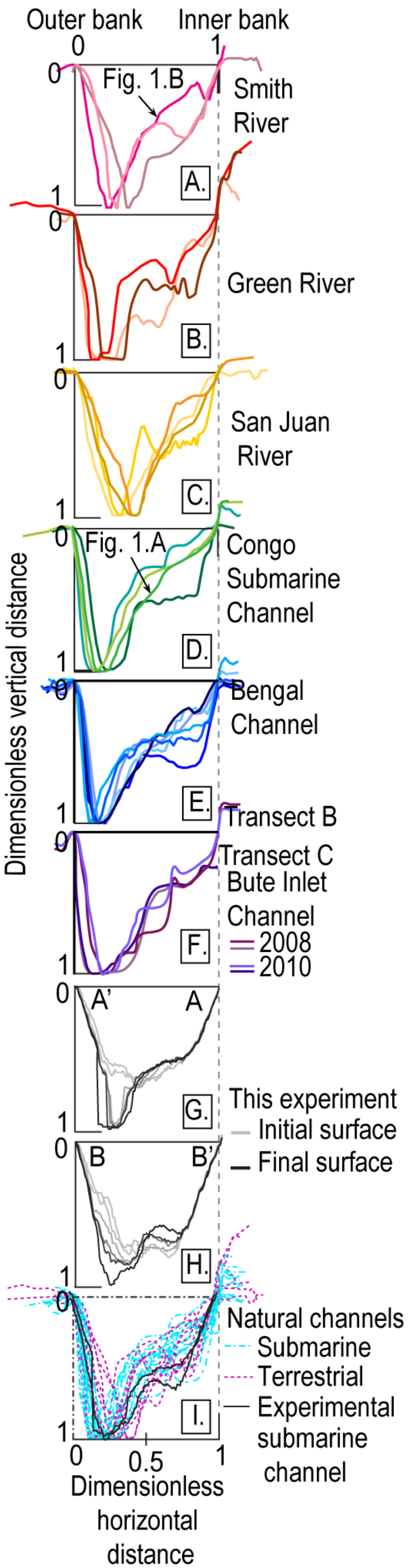


**Figure 5: Non-dimensionalized channel cross sections at bend apices in: A) Smith River, Oregon, B) Green River, Utah, C) San Juan River, Utah, D) the Congo submarine channel, Offshore Angola, E) the Bengal submarine channel, Bay of Bengal, F) the Bute submarine channel, British Columbia (from survey years 2008 and 2010), G, H) the submarine channel in our experiment at cross section A-A' and B-B' in Fig. 1A. Note: incision of the inner channel in our experiment was stalled when it reached the concrete platform 5 cm below the sediment bed. I) A comparison of cross-sections through natural and experimental channels in terrestrial and submarine settings show a remarkable similarity in the range of forms encountered at bend apices.**

## Methods

The experimental basin was 8m long, 6m wide and 2.0m deep. The sinuous channel was built with a weakly cohesive mixture of acrylic particles (specific gravity = 1.15; grain size data in supplementary Information) and clay (volumetric ratio: 10:1) on a sloping concrete ramp in a volumetric ratio of 10:1. The channel form was constructed from the dry sediment mixture and then slowly submerged. The channel was 45 cm wide at the top, 20 cm wide at the base, 14 cm deep and 2.5 m long, with a down-channel slope of approximately 7 degrees and 5 cm of erodible sediment on the channel bed. The channel was built upon a platform separated from the walls of the basin by deep moats that served to prevent currents from reflecting off the tank walls (basin schematic in supplementary information).

Five saline density currents with excess densities ~4% were released into the channel; the last three currents carried a 2% volumetric concentration of suspended acrylic sediment. Density currents were released into an experimental channel through a box with two perforated screens designed to extract momentum from flows. Density currents were ~10 cm thick and did not completely occupy the channel cross section. Saline fluid was not allowed to build-up in the basin during the experiment. Fluid was extracted through the floor drains as it flowed off the raised platform. The water level in the basin was maintained with a constant flux of fresh water and overflow drainage through a weir.

Salt (CaCl2) and water (and sediment, when it was used), were mixed together in a reservoir, until the salt was completely dissolved. The mixture was agitated over several hours and allowed to cool to room temperature (overnight), as the dissolution of this salt in water is an exothermic process. Once at room temperature, the mixture was pumped up to a constant head tank and then allowed to flow into the experimental basin at a controlled rate set by the constant hydraulic head and a system of valves. A generalized cross-section of the experimental basin used is shown in Figure SI1.

High-resolution bathymetry maps (vertical resolution ~100 microns; horizontal resolution = 4 mm), collected before and after each flow define changes wrought through erosion and deposition in the channel. We used a Vectrino Acoustic Doppler Velocimetric Profiler to map the flow field near the channel bed. The near-bed velocities were collected in 1mm vertical bins, and reported velocities were averaged over the time period of each experimental  run. Velocity data was averaged Continuous overhead and perspective time-lapse photographs, and video were collected during each experimental run. T channel was photograph after the passage of each current, once sediment in the water column had settled.

**References Cited**

1. Talling, P. J., Paull, C. K. & Piper, D. J. W. How are subaqueous sediment density flows triggered, what is their internal structure and how does it evolve? Direct observations from monitoring of active flows. *Earth-Sci. Rev.* **125,** 244–287 (2013).
2. Wynn, R. B., Cronin, B. T. & Peakall, J. Sinuous deep-water channels: Genesis, geometry and architecture. *Mar. Pet. Geol.* **24,** 341–387 (2007).
3. Deptuck, M. E., Sylvester, Z., Pirmez, C. & O'Byrne, C. Migration–aggradation history and 3-D seismic geomorphology of submarine channels in the Pleistocene Benin-major Canyon, western Niger Delta slope. *Mar. Pet. Geol.* **24,** 406–433 (2007).
4. Symons, W. O. *et al.* A new model for turbidity current behavior based on integration of flow monitoring and precision coring in a submarine canyon. *Geology* **45,** 367–370 (2017).
5. Azpiroz-Zabala, M. *et al.* Newly recognized turbidity current structure can explain prolonged flushing of submarine canyons. *Sci Adv* **3,** e1700200 (2017).
6. Hughes Clarke, J. E. First wide-angle view of channelized turbidity currents links migrating cyclic steps to flow characteristics. *Nat. Commun.* **7,** 11896 (2016).
7. Khripounoff, A. *et al.* Direct observation of intense turbidity current activity in the Zaire submarine valley at 4000 m water depth. *Mar. Geol.* **194,** 151–158 (2003).
8. Hay, A. E. Turbidity currents and submarine channel formation in Rupert Inlet, British Columbia: 1. Surge observations. *J. Geophys. Res.* **92,** 2875–2881 (1987).
9. Straub, K. M., Mohrig, D., McElroy, B. & Buttles, J. Interactions between turbidity currents and topography in aggrading sinuous submarine channels: A laboratory study. *Geological Society of America Bulletin* (2008).
10. Nakajima, T., Peakall, J., McCaffrey, W. D., Paton, D. A. & Thompson, P. J. P. Outer-Bank Bars: A New Intra-Channel Architectural Element within Sinuous Submarine Slope Channels. *J. Sediment. Res.* **79,** 872–886 (2009).

11. Métivier, F., Lajeunesse, E. & Cacas, M.-C. Submarine Canyons in the Bathtub. *J. Sediment. Res.* **75,** 6–11 (2005).

12. Mohrig, D. & Buttles, J. Deep turbidity currents in shallow channels. *Geology* **35,** 155–158 (2007).

13. Amos, K. J. *et al.* The influence of bend amplitude and planform morphology on flow and sedimentation in submarine channels. *Mar. Pet. Geol.* **27,** 1431–1447 (2010).

14. Janocko, M., Cartigny, M. B. J., Nemec, W. & Hansen, E. W. M. Turbidity current hydraulics and sediment deposition in erodible sinuous channels: Laboratory experiments and numerical simulations. *Mar. Pet. Geol.* **41,** 222–249 (2013).

15. de Leeuw, J., Eggenhuisen, J. T. & Cartigny, M. J. B. Morphodynamics of submarine channel inception revealed by new experimental approach. *Nat. Commun.* **7,** 10886 (2016).

16. Mitchell, N. C. Bedrock erosion by sedimentary flows in submarine canyons. *Geosphere* **10,** 892–904 (2014).

17. Whipple, K. X. Bedrock Rivers and the Geomorphology of Active Orogens. *Annu. Rev. Earth Planet. Sci.* **32,** 151–185 (2004).

18. Davis, W. M. The terraces of the Westfield River, Massachusetts. *Am. J. Sci.* **Series 414,** 77–94 (1902).

19. Pazzaglia, F. J. & Gardner, T. W. Fluvial terraces of the lower Susquehanna River. *Geomorphology* **8,** 83–113 (1993).

20. Hancock, G. S. & Anderson, R. S. Numerical modeling of fluvial strath-terrace formation in response to oscillating climate. *GSA Bulletin* **114,** 1131–1142 (2002).

21. Stark, C. P. *et al.* The climatic signature of incised river meanders. *Science* **327,** 1497–1501 (2010).

22. Finnegan, N. J. & Dietrich, W. E. Episodic bedrock strath terrace formation due to meander migration and cutoff. *Geology* **39,** 143–146 (2011).

23. Limaye, A. B. S. & Lamb, M. P. Numerical simulations of bedrock valley evolution by

meandering rivers with variable bank material. *Journal of Geophysical Research: Earth Surface* **119,** 927–950 (2014).

24. Shepard, F. P. Meander in valley crossing a deep-ocean fan. *Science* **154,** 385–386 (1966).
25. Babonneau, N., Savoye, B., Cremer, M. & Bez, M. Sedimentary Architecture in Meanders of a Submarine Channel: Detailed Study of the Present Congo Turbidite Channel (Zaiango Project). *J. Sediment. Res.* **80,** 852–866 (2010).
26. Conway, K. W., Barrie, J. V., Picard, K. & Bornhold, B. D. Submarine channel evolution: active channels in fjords, British Columbia, Canada. *Geo-Mar. Lett.* **32,** 301–312 (2012).
27. Maier, K. L. *et al.* Punctuated Deep-Water Channel Migration: High-Resolution Subsurface Data from the Lucia Chica Channel System, Offshore California, U.S.A. *J. Sediment. Res.* **82,** 1–8 (2012).

## Acknowledgements

For financial support, the authors acknowledge the Jackson School of Geosciences, the CSM-UT RioMAR Industry Consortium for financial support of this work, and The Oregon Department of Geology and Mineral Industries for the LiDAR data used in Fig 1..

## Author Contributions

A.M.F. conducted the experiments, compiled and analyzed data and was the lead author of the manuscript; D.M. provided significant editorial feed-back on the manuscript; J.B. assisted with experiments and data analyses and provided significant editorial feed-back on the manuscript.

## Competing Financial Interests

The authors declare no competing financial interests.

## <u>Supplementary Information</u>

### *Experiment Design*

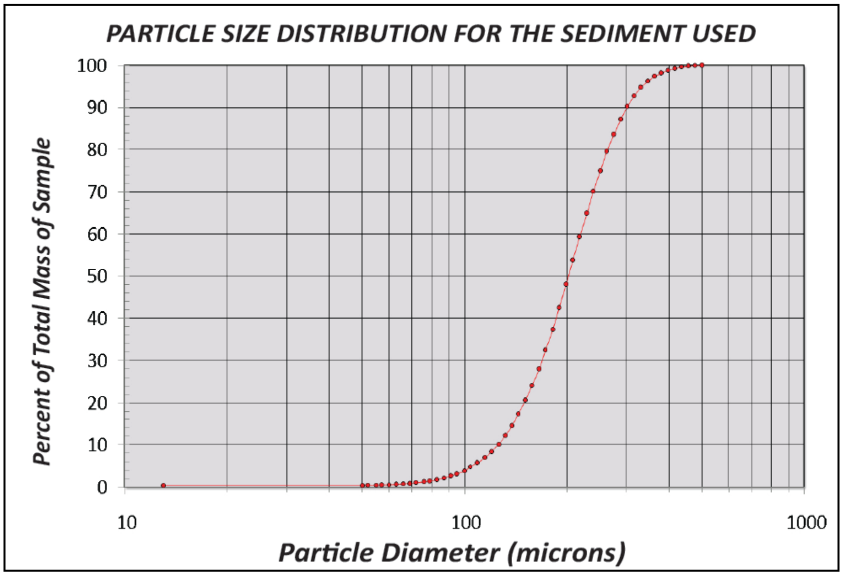


***Figure SI-1: The grain-size distribution of acrylic sediment used.***

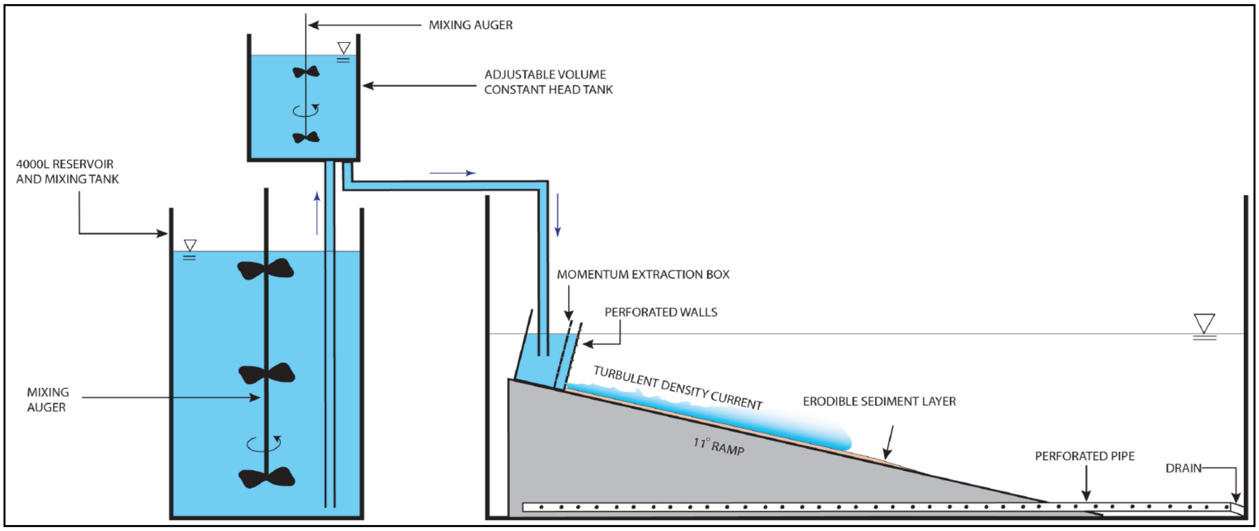


***Figure SI-2: A generalized schematic of the experimental basin***

***Dynamic Scaling***

This laboratory experiment can be roughly compared to natural systems through the scaling of three dimensionless variables, the densimetric Froude number (Frd), the Reynolds number (Re) and the ratio of particle fall velocity (ws) to current shear velocity (u*). An approximate dynamic similarity was assumed by setting Frd (lab) = Frd (prototype) [1]. Resulting prototype values of depth-averaged velocity, current thickness and flow duration are compiled in DR Table 1. Sediment transport properties are compared between experimental and natural systems by setting the ratio ws/u*(lab) equal to ws/u*(prototype). Values for ws were computed using the empirically derived relationship of ([2]). Shear velocities (u*) for the experimental currents were estimated as u*=(uCd)^½ where u is the depth averaged velocity of the density currents and Cd is the hydraulic drag coefficient approximated by the value 0.02 for experimental channels and 0.002 for natural channels[3,4]. Note: shear velocities estimated thus are greater than 3 times the estimated settling velocity of the D99 of acrylic particles used, indicating that particles were fully suspended once detached from the bed [5]. This quantitatively agrees with visual observations of transport patterns. Geometric and dynamic properties of the channels and currents, scaled approximately to natural systems, is shown in Table SI-1.

Table SI-1: Geometries and dynamics of experimental channel scaled to natural systems

| | | Experiment | Prototype |
|---|---|---|---|
| Geometric Scaling | channel depth | 0.15m | 50m |
| | channel width | 0.50m | 500m |

| | | | |
|---|---|---|---|
| Dynamic Scaling | depth averaged velocity | 0.10m/s | 1.83m/s |
| | shear velocity | 0.045m/s | 0.060m/s |
| | Fr d | 0.41 | 0.41 |
| | Re | 15000 | 6 x 107 |
| | Sediment composition and grain-size distribution (micron) | Acrylic D1=49 , D10=88 , D25=127, D50=146, D75=205, D90=243, D99=340 | Quartz. D1=19 , D10=33 , D25=47, D50=55, D75=75, D90=89, D99=124 |
| | flow duration | 25min | 40-72 minutes |
| | current thickness | ~0.10m | 33m |

***Topographic data***

Table SI-2: Data sources / locations for Figure 5

| | Terrestrial Channels | Coordinates of end points of cross-section | Source |
|---|---|---|---|
| 1 | Smith River1 | -123.7826371901627,43.80472633714489; -123.7746010278586,43.79981995552907 | Oregon Department of Geology and Mineral Industries |
| 2 | Smith River2 | -123.7604201127893,43.81115517323132; -123.7673292848834,43.79830226749066 | |
| 3 | Smith River3 | -123.6532970276423,43.81939479072555; -123.6600247308344,43.8065667856463 | |
| 4 | Green River1 | -109.6388033169158,38.58624113046864; -109.6419008067904,38.56505600805119 | Google Earth |
| 5 | Green River2 | -110.0523449828799,38.65642315320836; -110.0565156794953,38.63796866905698 | Google Earth |
| 6 | Green River3 | -109.8010734570593,38.31466238795997; -109.7542006529873,38.30187390633612 | Google Earth |
| 7 | Green River4 | -110.0856706426976,38.65581941640971; -110.0639219942443,38.6803400020592 | Google Earth |
| 8 | Colorado River | -110.908639822533,37.36145671781638; -110.8423561906744,37.33219665078475 | Google Earth |
| 9 | San Juan River1 | -109.7738676542044,37.21584872989421; -109.7526641747123,37.18948841812345 | Google Earth |
| 10 | San Juan River2 | -109.9189523741587,37.16557981421435; -109.9270346290523,37.1540908316806 | Google Earth |
| 11 | San Juan River3 | -109.7314943800335,37.20198777373232; -109.7401657271749,37.18926444104969 | Google Earth |

| | | | |
|---|---|---|---|
| 12 | San Juan River4 | -109.7763911352864,37.1900553535192; -109.7565150459447,37.18227160590539 | Google Earth |
| | Submarine Channels | Source | |
| 13 | Congo Channel1-4 | Babonneau et al., 2010[6] (Fig. 4, inset 1; Fig. 5 cross-sections; Fig. 7 cross-section | |
| 17 | Bengal Channel1-6 | Data provided by Tilmann Schwenk[7,8]. See data below. | |
| 19 | Bute Inlet Channel1-2 | Conway et al., 2013,[9] Fig. 6b | |

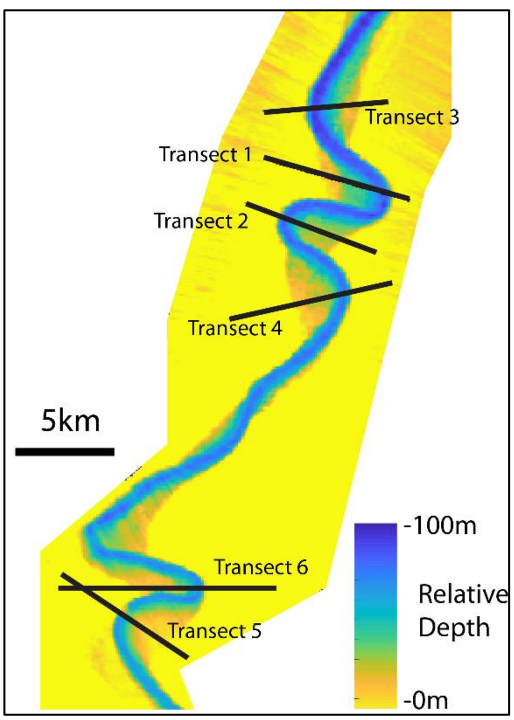


***Figure SI-3: Topographic data from the Bengal Channel***

Table SI-3: Bengal Channel cross sections used in Fig.5E

| X | Y | Z |
|---|---|---|
| Transect 1 | | |
| 3561.814 | 2764.549 | 499.4587 |
| 3562.088 | 2765.511 | 500.2395 |
| 3562.363 | 2766.472 | 500.2395 |
| 3562.638 | 2767.434 | 502.1104 |
| 3562.913 | 2768.395 | 502.0762 |
| 3563.187 | 2769.357 | 501.0259 |
| 3563.462 | 2770.319 | 499.7043 |
| 3563.737 | 2771.28 | 499.2727 |
| 3564.011 | 2772.242 | 500.728 |
| 3564.286 | 2773.203 | 501.323 |
| 3564.561 | 2774.165 | 501.2463 |
| 3564.836 | 2775.126 | 501.6074 |
| 3565.11 | 2776.088 | 501.7815 |
| 3565.385 | 2777.049 | 501.3899 |

| | | |
|---|---|---|
| 3565.66 | 2778.011 | 501.7163 |
| 3565.935 | 2778.972 | 503.8127 |
| 3566.209 | 2779.934 | 505.8171 |
| 3566.484 | 2780.895 | 505.4263 |
| 3566.759 | 2781.857 | 505.1541 |
| 3567.033 | 2782.818 | 505.019 |
| 3567.308 | 2783.78 | 506.4709 |
| 3567.583 | 2784.741 | 503.582 |
| 3567.858 | 2785.703 | 496.9043 |
| 3568.132 | 2786.664 | 487.2913 |
| 3568.407 | 2787.626 | 482.1067 |
| 3568.682 | 2788.587 | 484.4988 |
| 3568.956 | 2789.549 | 484.1414 |
| 3569.231 | 2790.511 | 485.6184 |
| 3569.506 | 2791.472 | 484.3679 |
| 3569.781 | 2792.434 | 485.4331 |
| 3570.055 | 2793.395 | 484.0623 |
| 3570.33 | 2794.357 | 478.2397 |

| | | |
|---|---|---|
| 3570.605 | 2795.318 | 478.0498 |
| 3570.879 | 2796.28 | 470.3757 |
| 3571.154 | 2797.241 | 466.5708 |
| 3571.429 | 2798.203 | 461.1531 |
| 3571.704 | 2799.164 | 460.3745 |
| 3571.978 | 2800.126 | 461.6633 |
| 3572.253 | 2801.087 | 460.79 |
| 3572.528 | 2802.049 | 461.573 |
| 3572.803 | 2803.01 | 461.2161 |
| 3573.077 | 2803.972 | 459.4604 |
| 3573.352 | 2804.933 | 455.8821 |
| 3573.627 | 2805.895 | 455.2827 |
| 3573.901 | 2806.856 | 451.5835 |
| 3574.176 | 2807.818 | 445.7292 |
| 3574.451 | 2808.779 | 438.8989 |
| 3574.726 | 2809.741 | 438.0415 |
| 3575 | 2810.703 | 435.6125 |
| 3575.275 | 2811.664 | 430.3228 |

| | | |
|---|---|---|
| 3575.55 | 2812.626 | 424.4956 |
| 3575.824 | 2813.587 | 421.238 |
| 3576.099 | 2814.549 | 419.8865 |
| 3576.374 | 2815.51 | 419.7874 |
| 3576.649 | 2816.472 | 419.0134 |
| 3576.923 | 2817.433 | 422.1704 |
| 3577.198 | 2818.395 | 433.8303 |
| 3577.473 | 2819.356 | 460.5615 |
| 3577.748 | 2820.318 | 486.6248 |
| 3578.022 | 2821.279 | 501.8035 |
| 3578.297 | 2822.241 | 502.1074 |
| 3578.572 | 2823.202 | 499.9741 |
| 3578.846 | 2824.164 | 499.4375 |
| 3579.121 | 2825.125 | 498.3967 |
| 3579.396 | 2826.087 | 496.7734 |
| 3579.671 | 2827.048 | 498.1201 |
| Transect 2 | | |
| 3580.808 | 2750.553 | 505.0867 |

| | | |
|---|---|---|
| 3581.156 | 2751.491 | 505.0867 |
| 3581.504 | 2752.428 | 503.8159 |
| 3581.852 | 2753.366 | 504.9336 |
| 3582.2 | 2754.303 | 505.1396 |
| 3582.547 | 2755.241 | 501.9661 |
| 3582.895 | 2756.179 | 502.2168 |
| 3583.243 | 2757.116 | 502.7256 |
| 3583.591 | 2758.054 | 500.7629 |
| 3583.939 | 2758.991 | 501.7971 |
| 3584.287 | 2759.929 | 506.5491 |
| 3584.634 | 2760.866 | 502.5356 |
| 3584.982 | 2761.804 | 503.3899 |
| 3585.33 | 2762.742 | 504.6633 |
| 3585.678 | 2763.679 | 504.491 |
| 3586.026 | 2764.617 | 506.3777 |
| 3586.373 | 2765.554 | 499.7292 |
| 3586.721 | 2766.492 | 494.3931 |
| 3587.069 | 2767.429 | 469.8796 |

| | | |
|---|---|---|
| 3587.417 | 2768.367 | 442.479 |
| 3587.765 | 2769.305 | 418.8752 |
| 3588.112 | 2770.242 | 417.1028 |
| 3588.46 | 2771.18 | 421.863 |
| 3588.808 | 2772.117 | 432.7422 |
| 3589.156 | 2773.055 | 438.373 |
| 3589.504 | 2773.992 | 446.8213 |
| 3589.851 | 2774.93 | 453.7612 |
| 3590.199 | 2775.868 | 457.0576 |
| 3590.547 | 2776.805 | 459.9719 |
| 3590.895 | 2777.743 | 457.7002 |
| 3591.243 | 2778.68 | 459.8496 |
| 3591.59 | 2779.618 | 465.2078 |
| 3591.938 | 2780.555 | 467.7456 |
| 3592.286 | 2781.493 | 467.7456 |
| 3592.634 | 2782.43 | 468.8381 |
| 3592.982 | 2783.368 | 470.0203 |
| 3593.33 | 2784.306 | 468.5266 |

| | | |
|---|---|---|
| 3593.677 | 2785.243 | 466.949 |
| 3594.025 | 2786.181 | 468.2185 |
| 3594.373 | 2787.118 | 468.8608 |
| 3594.721 | 2788.056 | 465.8953 |
| 3595.069 | 2788.993 | 470.0505 |
| 3595.416 | 2789.931 | 470.6814 |
| 3595.764 | 2790.869 | 469.5479 |
| 3596.112 | 2791.806 | 470.1123 |
| 3596.46 | 2792.744 | 468.7937 |
| 3596.808 | 2793.681 | 468.5659 |
| 3597.155 | 2794.619 | 471.7056 |
| 3597.503 | 2795.556 | 480.1018 |
| 3597.851 | 2796.494 | 480.1018 |
| 3598.199 | 2797.432 | 489.9429 |
| 3598.547 | 2798.369 | 506.3 |
| 3598.894 | 2799.307 | 506.0481 |
| 3599.242 | 2800.244 | 506.9702 |
| 3599.59 | 2801.182 | 506.2085 |

| | | |
|---|---|---|
| 3599.938 | 2802.119 | 506.8308 |
| 3600.286 | 2803.057 | 507.4011 |
| 3600.633 | 2803.995 | 502.7939 |
| 3600.981 | 2804.932 | 503.9058 |
| 3601.329 | 2805.87 | 504.3345 |
| 3601.677 | 2806.807 | 500.1052 |
| 3602.025 | 2807.745 | 500.7297 |
| 3602.372 | 2808.682 | 501.4092 |
| 3602.72 | 2809.62 | 499.7183 |
| 3603.068 | 2810.557 | 498.989 |
| 3603.416 | 2811.495 | 498.989 |
| 3603.764 | 2812.433 | 499.907 |
| Transect 3 | | |
| 3538.154 | 2758.884 | 492.3789 |
| 3538.086 | 2759.882 | 493.3291 |
| 3538.018 | 2760.88 | 494.3196 |
| 3537.951 | 2761.877 | 494.7246 |
| 3537.883 | 2762.875 | 496.821 |

| | | |
|---|---|---|
| 3537.815 | 2763.873 | 500.634 |
| 3537.748 | 2764.871 | 500.0891 |
| 3537.68 | 2765.868 | 498.2144 |
| 3537.612 | 2766.866 | 498.6411 |
| 3537.545 | 2767.864 | 499.9253 |
| 3537.477 | 2768.861 | 496.3804 |
| 3537.41 | 2769.859 | 496.0671 |
| 3537.342 | 2770.857 | 495.2263 |
| 3537.274 | 2771.854 | 495.3469 |
| 3537.207 | 2772.852 | 496.3381 |
| 3537.139 | 2773.85 | 496.2793 |
| 3537.071 | 2774.848 | 494.5564 |
| 3537.004 | 2775.845 | 495.2874 |
| 3536.936 | 2776.843 | 498.782 |
| 3536.868 | 2777.841 | 500.0381 |
| 3536.801 | 2778.838 | 489.6682 |
| 3536.733 | 2779.836 | 463.3796 |
| 3536.665 | 2780.834 | 433.0459 |

| | | |
|---|---|---|
| 3536.598 | 2781.832 | 416.0168 |
| 3536.53 | 2782.829 | 413.8276 |
| 3536.463 | 2783.827 | 414.3398 |
| 3536.395 | 2784.825 | 417.0977 |
| 3536.327 | 2785.822 | 422.9158 |
| 3536.26 | 2786.82 | 429.2554 |
| 3536.192 | 2787.818 | 434.5452 |
| 3536.124 | 2788.816 | 440.3308 |
| 3536.057 | 2789.813 | 444.801 |
| 3535.989 | 2790.811 | 448.0361 |
| 3535.921 | 2791.809 | 452.8691 |
| 3535.854 | 2792.806 | 458.342 |
| 3535.786 | 2793.804 | 465.0117 |
| 3535.718 | 2794.802 | 467.2815 |
| 3535.651 | 2795.8 | 466.825 |
| 3535.583 | 2796.797 | 472.5129 |
| 3535.516 | 2797.795 | 477.3623 |
| 3535.448 | 2798.793 | 480.0486 |

| | | |
|---|---|---|
| 3535.38 | 2799.79 | 482.4045 |
| 3535.313 | 2800.788 | 483.4497 |
| 3535.245 | 2801.786 | 480.4539 |
| 3535.177 | 2802.783 | 482.0789 |
| 3535.11 | 2803.781 | 486.8608 |
| 3535.042 | 2804.779 | 493.8394 |
| 3534.974 | 2805.777 | 498.7195 |
| 3534.907 | 2806.774 | 501.8169 |
| 3534.839 | 2807.772 | 498.8428 |
| 3534.771 | 2808.77 | 497.7661 |
| 3534.704 | 2809.767 | 497.9216 |
| 3534.636 | 2810.765 | 496.7517 |
| 3534.569 | 2811.763 | 498.2197 |
| 3534.501 | 2812.761 | 498.7166 |
| 3534.433 | 2813.758 | 497.5544 |
| 3534.366 | 2814.756 | 498.1433 |
| 3534.298 | 2815.754 | 497.1812 |
| 3534.23 | 2816.751 | 497.1885 |

| | | |
|---|---|---|
| 3534.163 | 2817.749 | 496.7751 |
| Transect 4 | | |
| 3635.46 | 2743.222 | 509.8472 |
| 3635.238 | 2744.197 | 511.429 |
| 3635.015 | 2745.172 | 511.2734 |
| 3634.793 | 2746.147 | 510.5366 |
| 3634.571 | 2747.122 | 509.3396 |
| 3634.348 | 2748.097 | 509.5215 |
| 3634.126 | 2749.072 | 509.6775 |
| 3633.904 | 2750.047 | 510.7617 |
| 3633.681 | 2751.022 | 513.7332 |
| 3633.459 | 2751.997 | 508.2424 |
| 3633.236 | 2752.972 | 508.3435 |
| 3633.014 | 2753.947 | 507.8877 |
| 3632.792 | 2754.921 | 507.0134 |
| 3632.569 | 2755.896 | 508.3696 |
| 3632.347 | 2756.871 | 508.5454 |
| 3632.125 | 2757.846 | 506.4949 |

| | | |
|---|---|---|
| 3631.902 | 2758.821 | 506.2175 |
| 3631.68 | 2759.796 | 507.4346 |
| 3631.458 | 2760.771 | 508.2148 |
| 3631.235 | 2761.746 | 510.0637 |
| 3631.013 | 2762.721 | 508.5295 |
| 3630.79 | 2763.696 | 504.9785 |
| 3630.568 | 2764.671 | 506.6875 |
| 3630.346 | 2765.646 | 509.3352 |
| 3630.123 | 2766.621 | 507.4846 |
| 3629.901 | 2767.596 | 506.5371 |
| 3629.679 | 2768.571 | 509.0146 |
| 3629.456 | 2769.546 | 508.5427 |
| 3629.234 | 2770.521 | 509.2092 |
| 3629.012 | 2771.496 | 509.2092 |
| 3628.789 | 2772.471 | 506.7678 |
| 3628.567 | 2773.446 | 500.9426 |
| 3628.345 | 2774.421 | 494.6709 |
| 3628.122 | 2775.396 | 491.1914 |

| | | |
|---|---|---|
| 3627.9 | 2776.371 | 490.79 |
| 3627.677 | 2777.346 | 490.759 |
| 3627.455 | 2778.321 | 487.0527 |
| 3627.233 | 2779.296 | 483.4392 |
| 3627.01 | 2780.271 | 480.6494 |
| 3626.788 | 2781.246 | 480.436 |
| 3626.566 | 2782.22 | 478.9146 |
| 3626.343 | 2783.195 | 476.7307 |
| 3626.121 | 2784.17 | 474.1692 |
| 3625.899 | 2785.145 | 472.187 |
| 3625.676 | 2786.12 | 470.781 |
| 3625.454 | 2787.095 | 475.3787 |
| 3625.231 | 2788.07 | 475.4653 |
| 3625.009 | 2789.045 | 472.719 |
| 3624.787 | 2790.02 | 471.9294 |
| 3624.564 | 2790.995 | 468.7434 |
| 3624.342 | 2791.97 | 463.4287 |
| 3624.12 | 2792.945 | 456.6833 |

| | | |
|---|---|---|
| 3623.897 | 2793.92 | 446.4316 |
| 3623.675 | 2794.895 | 434.4077 |
| 3623.453 | 2795.87 | 427.3394 |
| 3623.23 | 2796.845 | 425.7461 |
| 3623.008 | 2797.82 | 429.23 |
| 3622.786 | 2798.795 | 446.6494 |
| 3622.563 | 2799.77 | 472.7124 |
| 3622.341 | 2800.745 | 492.1047 |
| 3622.118 | 2801.72 | 506.2705 |
| 3621.896 | 2802.695 | 510.2144 |
| 3621.674 | 2803.67 | 506.2119 |
| 3621.451 | 2804.645 | 503.2959 |
| 3621.229 | 2805.62 | 503.0471 |
| 3621.007 | 2806.595 | 503.562 |
| 3620.784 | 2807.57 | 504.9954 |
| 3620.562 | 2808.545 | 505.6348 |
| 3620.34 | 2809.52 | 506.8853 |
| 3620.117 | 2810.494 | 506.8853 |

| | | |
|---|---|---|
| 3619.895 | 2811.469 | 504.8274 |
| 3619.672 | 2812.444 | 502.2617 |
| 3619.45 | 2813.419 | 501.7261 |
| 3619.228 | 2814.394 | 500.897 |
| 3619.005 | 2815.369 | 499.498 |
| 3618.783 | 2816.344 | 498.7126 |
| 3618.561 | 2817.319 | 498.3611 |
| 3618.338 | 2818.294 | 494.4478 |
| Transect 5 | | |
| 3761.092 | 2664.244 | 510.0837 |
| 3761.082 | 2665.244 | 509.9277 |
| 3761.072 | 2666.244 | 511.0129 |
| 3761.063 | 2667.244 | 507.6892 |
| 3761.053 | 2668.244 | 509.8535 |
| 3761.043 | 2669.244 | 513.2371 |
| 3761.033 | 2670.243 | 517.2832 |
| 3761.023 | 2671.243 | 517.1162 |
| 3761.013 | 2672.243 | 517.8604 |

| | | |
|---|---|---|
| 3761.003 | 2673.243 | 519.4021 |
| 3760.993 | 2674.243 | 519.5408 |
| 3760.984 | 2675.243 | 521.2952 |
| 3760.974 | 2676.243 | 521.4998 |
| 3760.964 | 2677.243 | 522.3289 |
| 3760.954 | 2678.243 | 523.9277 |
| 3760.944 | 2679.243 | 522.2039 |
| 3760.934 | 2680.243 | 522.1843 |
| 3760.924 | 2681.243 | 524.8862 |
| 3760.914 | 2682.243 | 526.2283 |
| 3760.905 | 2683.243 | 525.4902 |
| 3760.895 | 2684.243 | 523.3333 |
| 3760.885 | 2685.243 | 522.9604 |
| 3760.875 | 2686.243 | 523.6992 |
| 3760.865 | 2687.243 | 523.7522 |
| 3760.855 | 2688.243 | 523.8733 |
| 3760.845 | 2689.243 | 524.6152 |
| 3760.836 | 2690.243 | 526.0134 |

| | | |
|---|---|---|
| 3760.826 | 2691.242 | 528.0356 |
| 3760.816 | 2692.242 | 530.1946 |
| 3760.806 | 2693.242 | 530.7839 |
| 3760.796 | 2694.242 | 529.1428 |
| 3760.786 | 2695.242 | 530.2722 |
| 3760.776 | 2696.242 | 533.3503 |
| 3760.766 | 2697.242 | 529.6538 |
| 3760.757 | 2698.242 | 518.0305 |
| 3760.747 | 2699.242 | 503.6838 |
| 3760.737 | 2700.242 | 494.1946 |
| 3760.727 | 2701.242 | 491.074 |
| 3760.717 | 2702.242 | 490.0942 |
| 3760.707 | 2703.242 | 490.2227 |
| 3760.697 | 2704.242 | 489.6548 |
| 3760.688 | 2705.242 | 487.3076 |
| 3760.678 | 2706.242 | 487.3772 |
| 3760.668 | 2707.242 | 486.3489 |
| 3760.658 | 2708.242 | 485.1738 |

| | | |
|---|---|---|
| 3760.648 | 2709.242 | 485.0693 |
| 3760.638 | 2710.242 | 485.7356 |
| 3760.628 | 2711.241 | 483.345 |
| 3760.618 | 2712.241 | 484.228 |
| 3760.609 | 2713.241 | 484.5107 |
| 3760.599 | 2714.241 | 482.6208 |
| 3760.589 | 2715.241 | 479.9851 |
| 3760.579 | 2716.241 | 480.4297 |
| 3760.569 | 2717.241 | 478.333 |
| 3760.559 | 2718.241 | 476.2656 |
| 3760.549 | 2719.241 | 474.3916 |
| 3760.54 | 2720.241 | 475.2432 |
| 3760.53 | 2721.241 | 474.114 |
| 3760.52 | 2722.241 | 470.0115 |
| 3760.51 | 2723.241 | 466.0439 |
| 3760.5 | 2724.241 | 461.783 |
| 3760.49 | 2725.241 | 457.0117 |
| 3760.48 | 2726.241 | 453.0073 |

| | | |
|---|---|---|
| 3760.47 | 2727.241 | 449.2708 |
| 3760.461 | 2728.241 | 439.688 |
| 3760.451 | 2729.241 | 429.9866 |
| 3760.441 | 2730.241 | 427.614 |
| 3760.431 | 2731.241 | 446.1775 |
| 3760.421 | 2732.24 | 486.0601 |
| 3760.411 | 2733.24 | 514.52 |
| 3760.401 | 2734.24 | 519.6113 |
| 3760.391 | 2735.24 | 518.8157 |
| 3760.382 | 2736.24 | 519.6465 |
| 3760.372 | 2737.24 | 519.6323 |
| 3760.362 | 2738.24 | 517.5796 |
| 3760.352 | 2739.24 | 518.0757 |
| 3760.342 | 2740.24 | 519.5083 |
| 3760.332 | 2741.24 | 518.7087 |
| 3760.322 | 2742.24 | 518.4229 |
| 3760.313 | 2743.24 | 519.9045 |
| 3760.303 | 2744.24 | 522.5981 |

| | | |
|---|---|---|
| 3760.293 | 2745.24 | 524.2671 |
| 3760.283 | 2746.24 | 523.5745 |
| 3760.273 | 2747.24 | 521.5813 |
| 3760.263 | 2748.24 | 517.8965 |
| 3760.253 | 2749.24 | 513.0854 |
| 3760.243 | 2750.24 | 515.3662 |
| 3760.234 | 2751.24 | 517.978 |
| 3760.224 | 2752.239 | 518.75 |
| 3760.214 | 2753.239 | 515.8105 |
| 3760.204 | 2754.239 | 518.3206 |
| 3760.194 | 2755.239 | 521.0134 |
| 3760.184 | 2756.239 | 519.2241 |
| 3760.174 | 2757.239 | 517.5723 |
| 3760.165 | 2758.239 | 518.324 |
| 3760.155 | 2759.239 | 516.5085 |
| 3760.145 | 2760.239 | 514.6724 |
| 3760.135 | 2761.239 | 516.0088 |
| 3760.125 | 2762.239 | 515.4097 |

| | | |
|---|---|---|
| 3760.115 | 2763.239 | 512.7402 |
| 3760.105 | 2764.239 | 514.2402 |
| 3760.095 | 2765.239 | 516.7664 |
| Transect 6 | | |
| 3793.083 | 2724.894 | 531.3044 |
| 3792.543 | 2724.052 | 532.7021 |
| 3792.002 | 2723.211 | 532.8149 |
| 3791.462 | 2722.37 | 531.7319 |
| 3790.921 | 2721.528 | 531.7319 |
| 3790.381 | 2720.687 | 533.0977 |
| 3789.84 | 2719.846 | 531.6421 |
| 3789.3 | 2719.004 | 532.5063 |
| 3788.759 | 2718.163 | 533.1738 |
| 3788.219 | 2717.322 | 531.2031 |
| 3787.678 | 2716.48 | 520.9128 |
| 3787.138 | 2715.639 | 509.6631 |
| 3786.597 | 2714.798 | 498.251 |
| 3786.057 | 2713.956 | 491.5867 |

| | | |
|---|---|---|
| 3785.516 | 2713.115 | 489.1787 |
| 3784.975 | 2712.274 | 488.7603 |
| 3784.435 | 2711.432 | 487.9541 |
| 3783.894 | 2710.591 | 487.9541 |
| 3783.354 | 2709.75 | 488.8 |
| 3782.813 | 2708.908 | 490.8989 |
| 3782.273 | 2708.067 | 491.5117 |
| 3781.732 | 2707.226 | 493.5405 |
| 3781.192 | 2706.384 | 494.5083 |
| 3780.651 | 2705.543 | 494.5083 |
| 3780.111 | 2704.702 | 494.3167 |
| 3779.57 | 2703.86 | 494.7908 |
| 3779.03 | 2703.019 | 495.5085 |
| 3778.489 | 2702.178 | 489.1948 |
| 3777.949 | 2701.336 | 483.4529 |
| 3777.408 | 2700.495 | 477.3682 |
| 3776.868 | 2699.654 | 477.3682 |
| 3776.327 | 2698.812 | 471.3027 |

| | | |
|---|---|---|
| 3775.787 | 2697.971 | 466.5161 |
| 3775.246 | 2697.13 | 461.7769 |
| 3774.706 | 2696.288 | 457.708 |
| 3774.165 | 2695.447 | 458.0515 |
| 3773.625 | 2694.606 | 458.0515 |
| 3773.084 | 2693.764 | 466.7202 |
| 3772.544 | 2692.923 | 470.5908 |
| 3772.003 | 2692.082 | 503.4775 |
| 3771.462 | 2691.24 | 530.6262 |
| 3770.922 | 2690.399 | 535.4709 |
| 3770.381 | 2689.558 | 532.7119 |
| 3769.841 | 2688.716 | 527.9897 |
| 3769.3 | 2687.875 | 528.2622 |
| 3768.76 | 2687.034 | 530.4871 |
| 3768.219 | 2686.192 | 531.8411 |
| 3767.679 | 2685.351 | 529.2329 |
| 3767.138 | 2684.51 | 529.1648 |
| 3766.598 | 2683.668 | 526.8899 |

| | | |
|---|---|---|
| 3766.057 | 2682.827 | 527.0752 |
| 3765.517 | 2681.986 | 526.438 |
| 3764.976 | 2681.144 | 525.1165 |
| 3764.436 | 2680.303 | 522.7183 |
| 3763.895 | 2679.462 | 522.574 |
| 3763.355 | 2678.62 | 521.6746 |
| 3762.814 | 2677.779 | 520.2239 |
| 3762.274 | 2676.938 | 521.7698 |
| 3761.733 | 2676.096 | 521.3103 |
| 3761.193 | 2675.255 | 521.2952 |
| 3760.652 | 2674.414 | 519.5408 |
| 3760.112 | 2673.572 | 519.9771 |
| 3759.571 | 2672.731 | 518.1797 |
| 3759.031 | 2671.89 | 518.3035 |
| 3758.49 | 2671.048 | 518.2732 |
| 3757.949 | 2670.207 | 516.6565 |
| 3757.409 | 2669.366 | 515.6716 |
| 3756.868 | 2668.525 | 515.6716 |

| | | |
|---|---|---|
| 3756.328 | 2667.683 | 516.7539 |
| 3755.787 | 2666.842 | 515.3152 |
| 3755.247 | 2666.001 | 511.0154 |

**References cited**


1. Graf, W. H. Hydraulics of sediment transport, Series in water resources and environmental engineering. (1971).
2. Dietrich, W. E. Settling velocity of natural particles. *Water Resour. Res.* **18,** 1615–1626 (1982).
3. Parker, G., Garcia, M., Fukushima, Y. & Yu, W. Experiments on turbidity currents over an erodible bed. *J. Hydraul. Res.* **25,** 123–147 (1987).
4. Garcia Marcelo H. Depositional Turbidity Currents Laden with Poorly Sorted Sediment. *J. Hydraul. Eng.* **120,** 1240–1263 (1994).
5. Smith, J. D. & Hopkins, T. S. *Sediment Transport on the Continental Shelf Off Washington and Oregon in Light of Recent Current Measurements*. (Washington Univ., Seattle. Dept. of Oceanography. Atomic Energy Commission, Athens (Greece), 1971).
6. Babonneau, N., Savoye, B., Cremer, M. & Bez, M. Sedimentary Architecture in Meanders of a Submarine Channel: Detailed Study of the Present Congo Turbidite Channel (Zaiango Project). *J. Sediment. Res.* **80,** 852–866 (2010).
7. Schwenk, T., Speiß, V., Hübscher, C. & Breitzke, M. Frequent channel avulsions within the active channel--levee system of the middle Bengal Fan—an exceptional channel--levee development derived from Parasound and Hydrosweep data: Deep-Sea Research II, v. 50. *Deep-Sea Res.* **50,** 1023–1045 (2003).

8. Schwenk, T., Spiess, V., Breitzke, M. & Huebscher, C. The architecture and evolution of the Middle Bengal Fan in vicinity of the active channel–levee system imaged by high-resolution seismic data. **22,** 637–656 (2005).
9. Conway, K. W., Barrie, J. V., Picard, K. & Bornhold, B. D. Submarine channel evolution: active channels in fjords, British Columbia, Canada. *Geo-Mar. Lett.* **32,** 301–312 (2012).